



Title	Nuclear retention of STAT3 through the coiled-coil domain regulates its activity.
Author(s)	Sato, Noriko; Tsuruma, Rieko; Imoto, Seiyu; Sekine, Yuichi; Muromoto, Ryuta; Sugiyama, Kenji; Matsuda, Tadashi
Citation	Biochemical and Biophysical Research Communications, 336(2), 617-624 https://doi.org/10.1016/j.bbrc.2005.08.145
Issue Date	2005-10-21
Doc URL	http://hdl.handle.net/2115/22106
Type	article (author version)
File Information	BBRC336-2.pdf



[Instructions for use](#)

Title: Nuclear retention of STAT3 through the coiled-coil domain regulates its activity

Authors: Noriko Sato*†, Rieko Tsuruma *†, Seiyu Imoto*, Yuichi Sekine*, Ryuta Muromoto*, Kenji Sugiyama# and Tadashi Matsuda*

Affiliation: *Department of Immunology, Graduate School of Pharmaceutical Sciences, Hokkaido University, Kita-Ku Kita 12 Nishi 6, Sapporo 060-0812, Japan, #Nippon Boehringer Ingelheim Co., Ltd., Kawanishi Pharma Research Institute, 3-10-1 Yato, Kawanishi, Hyogo 666-0193, Japan

†These authors contributed equally to this work.

Footnotes: This work was supported in part by grants from the Osaka Foundation for Promotion of Clinical Immunology, the Naito Foundation, the Akiyama Foundation and the Ichiro Kanehara Foundation.

Address correspondence to: Dr. Tadashi Matsuda, Department of Immunology, Graduate School of Pharmaceutical Sciences, Hokkaido University, Kita-ku Kita 12 Nishi 6, Sapporo 060-0812, Japan TEL: 81-11-706-3243, FAX: 81-11-706-4990, E-mail: tmatsuda@pharm.hokudai.ac.jp

Running title: Nuclear retention of STAT3 regulates STAT3 activity

Key words: IL-6; LIF; STAT3; nuclear translocation; phosphorylation; transcription

Abstract

Signal transducer and activator of transcription 3 (STAT3), which mediates biological actions in many physiological processes, is activated by cytokines and growth factors via specific tyrosine phosphorylation, dimerization and nuclear translocation. However, the mechanism involved in its nuclear translocation remains unclear. A previous study demonstrated that STAT3 with Arg-214/215 mutations in the coiled-coil domain (R214A/R215A; STAT3 RA) failed to undergo nuclear translocation. Here, we re-examined the nature of the STAT3 RA mutant and found that it showed higher and more extensive tyrosine-phosphorylation as well as much higher STAT3 transcriptional activity in response to stimuli. Furthermore, STAT3 RA showed nuclear translocation and faster nuclear export than wild-type STAT3 after stimulation. Moreover, nuclear retention of STAT3 RA by a chromosomal region maintenance 1 (CRM1) inhibitor, leptomycin B, decreased the enhanced STAT3 activation by stimuli. These data demonstrate that Arg-214/215 are involved in CRM1-mediated STAT3 nuclear export and the regulation of STAT3 activity.

Introduction

The Jak/signal transducers and activators of transcription (STAT) pathways are utilized by a wide range of cytokines to regulate gene expression. Cytokines activate members of the Jak family of protein tyrosine kinases, which in turn activate one or more of the STAT family of transcription factors by tyrosine phosphorylation. STATs are unusual among transcription factors in that they have the characteristics of cytoplasmic signaling molecules, including a Src-homology 2 (SH2) domain and tyrosine phosphorylation sites. Upon tyrosine phosphorylation in response to receptor activation, STATs dimerize through interactions of their SH2 domain with phosphorylated tyrosine residues and translocate to the nucleus (1, 2, 3, 4). In recent years, constitutive or dysregulated STAT expressions have been identified in cancer cells and oncogene-transfected cells, and also shown to be involved in a wide range of other diseases, including autoimmune diseases (5, 6, 7, 8).

To date, seven different STAT genes have been identified in mammals. The encoded proteins vary in length from 750-850 amino acid residues and share 20-50% pairwise sequence identity. In general, STAT proteins bind as dimers to target DNA sites with a 9-base-pair (bp) consensus sequence (2).

The crystal structures of STAT proteins revealed several conserved functional domains, including the N-terminal domain, coiled-coil domain, DNA binding domain and linker domain, followed by the SH2 domain and C-terminal transactivation domain (9, 10, 11). Although nuclear translocation is critical for STAT activation, no classical nuclear localization signals (NLSs) have been identified in STAT proteins, and the mechanisms of their nuclear import remain unclear.

Recently, an arginine/lysine-rich element in the DNA binding domain of STAT1 was reported to be important for interferon-induced nuclear import of STAT1 and STAT2 (12, 13). In addition, leucine 407 in the DNA binding domain of STAT1 is required for its nuclear import (14). Furthermore, importin- β 5 (NPI-1) interacts with STAT1 homodimers and STAT1/STAT2 heterodimers and is involved in their nuclear import (14, 15, 16). A sequence in the DNA binding domain of STAT5b is necessary for the nuclear translocation induced by growth hormone (17). Recently, two sequence clusters located in the coiled-coil domain and DNA binding domain of STAT3 were found to be necessary for epidermal growth factor (EGF)- or interleukin (IL)-6-induced nuclear translocation (18). Furthermore, STAT3 mutants with Arg-214/215 or Arg-414/417 mutations in these domains underwent tyrosine-phosphorylation but failed to enter the nucleus in response to EGF or IL-6. However, the precise molecular mechanisms of the nuclear translocation of STAT3 remain largely unclear.

In this study, we used a nuclear translocation-defective mutant in which Arg 214 and Arg 215 were substituted with Ala (STAT3 R214/215A; STAT3 RA) to clarify the mechanisms of STAT3 nuclear translocation. Importantly, we found that STAT3 RA translocated into the nucleus and demonstrated markedly enhanced STAT3-mediated transcriptional activity as well as IL-6- or leukemia inhibitory factor (LIF)-induced tyrosine-phosphorylation compared with endogenous STAT3. Furthermore, STAT3 RA showed faster nuclear export than wild-type STAT3 (STAT3 WT) after stimulation. Moreover, nuclear accumulation of STAT3 RA by a chromosomal region maintenance 1 (CRM1) inhibitor, leptomycin B (LMB), decreased the enhanced STAT3 activation

by stimuli. These findings provide novel clues toward determining the precise mechanisms of STAT3 nuclear localization and its regulation within the nucleus.

Materials and Methods

Reagents and antibodies

Recombinant human IL-6 and interferon (IFN)- α were kindly provided from Ajinomoto (Tokyo, Japan) and Sumitomo Pharmaceuticals (Osaka, Japan), respectively. Recombinant human LIF was purchased from INTERGEN (Purchase, NY). LMB was a kind gift from Dr. M. Yoshida (19)(Riken, Wako, Japan). Expression vectors, epitope-tagged STAT3, STAT3 YF and STAT3-LUC, ISRE-LUC, were provided by Dr. T. Hirano (Osaka University, Osaka, Japan) (20). Expression vectors for epitope-tagged STAT3 RA mutant was generated by PCR methods and sequenced (16, primer sequences are available upon request). Anti-CRM1, -STAT3 and -c-Myc were obtained from Santa Cruz Biotechnology (Santa Cruz, CA, USA). Anti-FLAG mAb (M2) was from Sigma-Aldrich (Saint Louis, MO, USA). Anti-phospho-STAT3 (pSTAT3) Tyr705 was purchased from Cell Signaling Technologies (Beverly, MA). Fluorescein isothiocyanate (FITC)-conjugated anti-rabbit IgG and rhodamine-conjugated anti-mouse IgG was purchased from Chemicon (Temecula, CA).

Cell culture, transfection, and luciferase assays

Human embryonic kidney carcinoma cell line, 293T, was maintained in DMEM containing 10% FCS and transfected by the standard calcium precipitation protocol (21). The cells were harvested 36 hrs after transfection and lysed in 100 μ l of Reporter Lysis Buffer (Promega, Madison, WI) and

assayed for luciferase and β -galactosidase activities according to the manufacturer's instructions. Luciferase activities were normalized to the β -galactosidase activities. Three or more independent experiments were carried out for each assay. Human hepatoma cell line Hep3B was maintained in DMEM containing 10 % FCS. Before stimulation, the cells were cultured for 12 hrs in DMEM containing 1% FCS followed by treatment with IL-6. Hep3B cells in a 12-well plate were transfected with using jetPEI (PolyPlus-transfection, Strasbourg, France) according to the manufacturer's instructions. The cells were harvested and assayed for the luciferase activity using the Dual-Luciferase Reporter Assay System (Promega, Madison, WI) according to the manufacturer's instructions. At least three independent experiments were carried out for each assay.

Immunoprecipitation and immunoblotting

The immunoprecipitation and Western blotting assays were performed as described previously (22). Cells were harvested and lysed in lysis buffer (50 mM Tris-HCl, pH 7.4, 0.15 M NaCl, containing 1% NP-40, 1 mM sodium orthovanadate, 1 mM phenylmethylsulfonyl fluoride and 10 mg/ml each of aprotinin, pepstatin and leupeptin). The immunoprecipitates from cell lysates were resolved on 5-20% SDS-PAGE and transferred to Immobilon filter (Millipore; Bedford, MA). The filters were then immunoblotted with each antibody. Immunoreactive proteins were visualized using an enhanced chemiluminescence detection system (Amersham Pharmacia Biotech).

Indirect Immunofluorescence

Hep3B cells were maintained in DMEM containing 10% FCS transfected with Myc-STAT3 WT or Myc-STAT3 RA mutant by using jetPEI. Thirty hrs after transfection, the cells were stimulated by IL-6 (50 ng/ml) for the indicated periods. After IL-6-stimulation, the cells were fixed with a solution containing 4% paraformaldehyde, permeabilized with 1 % Triton-X in PBS and reacted with rabbit anti-FLAG antibody and/or mouse anti-Myc antibody as described previously (23). The cells were then reacted with fluorescein isothiocyanate (FITC)-conjugated anti-rabbit IgG and/or rhodamine-conjugated anti-mouse IgG (Chemicon, Temecula, CA, USA) and observed under a confocal laser fluorescent microscope. At the same time, the nuclei in the cells were stained with 4',6-diamidino-2-phenylindole (DAPI) (Wako, Tokyo, Japan). Images were obtained by using a Zeiss LSM 510 laser scanning microscope with an Apochromat x63/1.4 oil immersion objective and x4 zoom.

Results and Discussion

Enhanced STAT3-mediated transcriptional activation by the STAT3 RA mutant

Previous studies demonstrated that α -helix 2 in the coiled-coil domain contains a potential NLS for nuclear localization using a series of deletion mutants. The coiled-coil domain is composed of four antiparallel α -helices, of which two are long (α 1 and α 2) and two are short (α 3 and α 4) (10). Furthermore, STAT3 RA with mutations in α -helix 2 within the coiled-coil domain failed to translocate from the cytoplasm to the nucleus after EGF or IL-6 treatment (18). To identify the molecular mechanisms of the nuclear translocation of STAT3, we re-examined the nature of this STAT3 RA mutant. Since STAT3 RA was reported to be a nuclear translocation-defective mutant, we first examined whether it acted as a dominant-negative form of STAT3, similar to the case for STAT3 YF, in which a critical tyrosine (Tyr705) for STAT3 activation is substituted with phenylalanine. To this end, we performed transient transfection assays using 293T or Hep3B cells. The IL-6/STAT3-mediated transcriptional responses were measured using STAT3-LUC, in which the α 2-macroglobulin promoter drives the expression of a luciferase (LUC) reporter gene. 293T cells were transfected with STAT3-LUC together with STAT3 WT, STAT3 RA or STAT3 YF. After 36 h, cells were treated with LIF for 8 h and the LUC activities were determined. Unexpectedly, when cells were co-transfected with STAT3 RA, but not STAT3 WT or STAT3 YF, the transcriptional activation of STAT3-LUC was markedly augmented in a dose-dependent manner (Fig. 1A, B and C). In contrast, co-expression of STAT3 YF inhibited STAT3-LUC in a

dose-dependent manner (Fig. 1C). Similar results were obtained from transient transcription assays using an IL-6-responsive human hepatoma cell line, Hep3B (Fig. 1D). Next, we examined the effect of STAT3 RA on the STAT1-mediated signaling pathway by measuring the IFN/STAT1-mediated transcriptional responses via interferon-stimulated response element (ISRE)-mediated expression of the LUC reporter gene. As shown in Fig. 1E, expression of STAT3 RA had no effect on the IFN/STAT1-mediated ISRE-LUC activity. Consistent with the above findings, a previous report demonstrated that STAT3 RA formed homodimers and bound strongly to DNA, since DNA-STAT3 RA complexes were supershifted by an anti-STAT3 antibody. These results indicate that the transcriptional activity of STAT3 RA becomes hyperactivated in response to ligand stimulation.

STAT3 RA transfection induces enhanced phosphorylation of endogenous STAT3 and ectopically-expressed STAT3 RA after LIF stimulation

Next, we examined whether the phosphorylation of STAT3, which triggers its activation, was altered in the STAT3 RA mutant. 293T cells were transfected with Myc-tagged STAT3 WT or STAT3 RA, and then lysed and immunoprecipitated with an anti-Myc antibody. The immunoprecipitates obtained were blotted with anti-pSTAT3 Tyr705 or anti-Myc antibody. Time course analyses revealed that, upon expression of STAT3 RA, LIF-induced tyrosine-phosphorylation of STAT3 was remarkably enhanced and sustained for 3 h, compared with that of STAT3 WT transfectants (Fig. 2A). Comparable expressions of STAT3 WT and STAT3 RA were

confirmed by immunoblotting with the anti-Myc antibody. To further assess the phosphorylation of endogenous STAT3, we performed western blot analyses using aliquots of the total cell lysates from the transfectants. As shown in Fig. 2B, tyrosine-phosphorylation of endogenous STAT3 in the total cell lysates was also enhanced and extensively sustained in the STAT3 RA-transfected 293T cells, similar to the results for STAT3 RA in the immunoprecipitates obtained with the anti-Myc antibody (Fig. 2A). These data indicate that STAT3 RA transfection induced enhanced phosphorylation of both endogenous STAT3 and ectopically-expressed STAT3 RA, and augmented LIF-mediated STAT3 transcriptional activation in 293T cells.

STAT3 RA is mainly localized at the nuclear rim and merges with CRM1 in Hep3B cells after IL-6 stimulation

We further examined how IL-6 stimulation affects the subcellular localizations of STAT3 WT and STAT3 RA. An expression vector for Myc-tagged STAT3 WT or STAT3 RA was transfected into Hep3B cells. At 24 h after the transfection, the cells were left untreated or treated with IL-6, then fixed, reacted with anti-Myc and anti-pSTAT3 Tyr705 antibodies and visualized with a rhodamine- or FITC-conjugated secondary antibody. As shown in Fig. 3A, STAT3 WT and STAT3 RA were both localized in the cytoplasm without IL-6 stimulation. After 30 min of IL-6 stimulation, STAT3 WT was translocated into the nucleus and stained with the anti-pSTAT3 antibody. However, STAT3 RA mainly remained in the cytoplasm, consistent with a previous report. Importantly, we observed strong staining of STAT3 RA at the nuclear rim region after IL-6 stimulation (Fig. 3A,

lower right panel). Furthermore, the same region and the nucleus were strongly stained with the anti-pSTAT3 antibody. These results indicate that STAT3 RA failed to localize in the nucleus, although both endogenous STAT3 and ectopically-expressed STAT3 RA were strongly tyrosine-phosphorylated after IL-6 stimulation. These results also suggested that nuclear phosphatases were unable to access STAT3 RA or endogenous STAT3 in the presence of STAT3 RA. To confirm this possibility, we tested the interaction between STAT3 and a STAT3 nuclear phosphatase, TC-PTP (24). When we examined the binding potentials of STAT3 WT and STAT3 RA to a substrate-trapping mutant, TC-PTP Asp/Ala (D/A), which is a catalytically inactive form of TC-PTP, no significant difference was observed (data not shown), suggesting that the tyrosine-hyperphosphorylation of STAT3 by STAT3 RA is not due to inaccessibility of STAT3 to TC-PTP. However, we cannot currently exclude the possibility that other unknown nuclear phosphatases may be involved in this process.

To further address the localization of STAT3 RA at the nuclear rim region, we examined the co-localization of STAT3 RA with CRM1, which shows punctate staining of the nuclear rim and has the characteristic staining pattern of a nuclear pore complex protein (25). CRM1 is also involved in the nuclear export of STAT3 (26, 27). As shown in Fig. 3B, CRM1 was localized at the nuclear rim region with or without IL-6 stimulation. After IL-6 stimulation, STAT3 RA, but not STAT3 WT, was localized at the nuclear rim region and strongly merged with CRM1 (Fig. 3B, lower right panel). These findings also support that STAT3 RA is a nuclear translocation-defective mutant that co-localizes with nuclear pore complex proteins such as CRM1.

To further confirm this fact, we carried out time course analyses of the subcellular localizations of STAT3 WT and STAT3 RA in Hep3B cells after IL-6 stimulation. Surprisingly, the data demonstrated that STAT RA was localized within the nucleus, rather than at the nuclear rim region, at 15 min after the IL-6 stimulation (Fig. 4A), suggesting that STAT3 RA was initially imported into the nucleus and then immediately exported into the cytoplasm. Next, we investigated the effect of the CRM1 inhibitor LMB on STAT3 RA localization after IL-6 stimulation. LMB treatment is known to inhibit STAT3 nuclear export by binding to the CRM1 shuttling receptor (26, 27). As shown in Fig. 4B, LMB treatment resulted in nuclear accumulation of STAT3 RA as well as STAT3 WT. These data emphasize that STAT3 RA is not a nuclear localization-defective mutant.

Nuclear retention of STAT3 RA decreases its enhanced STAT3 activation by stimuli

Finally, we examined whether the nuclear retention of STAT3 RA by LMB affected the enhanced STAT3 activation by STAT3 RA. To this end, we performed transient transfection assays of 293T or Hep3B cells using STAT3-LUC in the absence or presence of LMB. Consistent with the above results (Fig. 1B and D), expression of STAT3 RA enhanced the STAT3 activity in both 293T and Hep3B cells. However, the enhanced STAT3 activity induced by STAT3 RA was inhibited by treatment with LMB (Fig. 4B). These results indicate that correct nuclear retention of STAT3 regulates its transcriptional activity. We finally examined the binding potential of STAT3 RA or STAT3 WT to CRM1. 293T cells were transfected with Myc-tagged STAT3 WT or STAT3 RA. The cells were stimulated with LIF and then lysed and immunoprecipitated with an anti-Myc

antibody. The immunoprecipitates obtained were blotted with anti-CRM1 or anti-Myc antibody. As shown in Fig. 4D, the immunoprecipitates contained CRM1 proteins. Importantly, the immunoprecipitates from the STAT3 RA-transfectants contained much more CRM1 proteins, indicating that STAT3 RA shows stronger binding potential to CRM1.

Concluding remarks

During the process of IL-6/LIF-mediated transcriptional activation of STAT3, STAT3 proteins translocate into the nucleus and are subsequently exported from the nucleus in a CRM1-dependent manner (26, 27). This study provides evidence that Arg-214/215 in the coiled-coil domain of STAT3 is involved in enhancement of transcriptional activation of STAT3 by hyperphosphorylation of both ectopically expressed STAT3 RA and endogenous STAT3. Interestingly, ectopically expression of STAT3 RA enhanced phosphorylation of both STAT3 RA and endogenous STAT3 (Fig, 2B). The data in Fig. 3A demonstrate that a rapid export of STAT3 RA may inhibits export of endogenous STAT3 and tyrosine-phosphorylated endogenous STAT3 is accumulated in the nucleus. This is one of the mechanisms why STAT3 RA expression enhances phosphorylation of both STAT3 RA and endogenous STAT3. Another mechanism is an inhibition of STAT3 dephosphorylation by STAT3 RA in the nucleus. Indeed, LIF-induced phosphorylated STAT3 WT and STAT3 RA were dephosphorylated by expression of TC-PTP in 293T cells. However, hyperphosphorylated STAT3 RA showed a good resistance against dephosphorylation by TC-PTP in 293T cells (data not shown), suggesting trapping of endogenous TC-PTP by STAT3

RA induces enhanced phosphorylation of endogenous STAT3, although the binding potentials of STAT3 WT and STAT3 RA to TC-PTPD/A were almost similar as mentioned above.

It has been previously demonstrated that a homodimer formation of STAT3 RA is so abundant and a heterodimer formation between STAT3 RA and endogenous STAT1 is not detectable, when STAT3 RA was expressed in monkey COS-1 cells (18). This data suggest that STAT3 RA shows a stronger dimer formation than STAT3 WT. When we coexpressed epitope-tagged STAT3 WT and STAT3 RA in 293T cells, a dimer formation between STAT3 WT and STAT3 RA was observed. However, a dimer formation between STAT3 WT and STAT3 WT was much abundant. Furthermore, a dimer formation between STAT3 RA and STAT3 RA was similarly abundant. We could not detect a dimer formation between STAT3 RA and endogenous STAT3. Moreover, any significant difference in the capacity of a dimer formation of STAT3 WT or STAT3 RA was not observed (data not shown), indicating that enhanced STAT3 activity of STAT3 RA is not due to its strong dimer formation.

This study also show that Arg-214/215 of STAT3 is important for a correct interactions with the nuclear export machineries, including CRM1, that lead to the nuclear export of STAT3. Indeed, STAT3 RA interacted with CRM1 stronger than STAT3 WT (Fig. 4D). A Ras-like small GTPase, Ran may also play a crucial role in the nuclear shuttling of STAT3. A dominant negative form of Ran, Ran T24N, which has low GTP and GDP binding affinity and inhibits RCC1 exchange activity (28), suppressed the STAT3 activation (N. Sato and R. Tsuruma, unpublished data).

Our present results indicate a novel physiological role of the nuclear retention of STAT3 in IL-

6/LIF-mediated transcriptional regulation. Thus, manipulation of STAT3 nuclear retention is likely to provide a novel therapeutic strategy for several cancers carrying constitutively activated STAT3.

Acknowledgements

We thank Dr. T. Hirano and Dr. M Yoshida for their kind gifts of reagents.

References

1. J. E. Darnell Jr., I. M. Kerr and G. R. Stark, Jak-STAT pathways and transcriptional activation in response to IFNs and other extracellular signaling proteins. *Science* **264** (1994) 1415-1421.
2. J. N. Ihle, STATs: signal transducers and activators of transcription. *Cell* **84** (1996) 331-334.
3. J. J. O'Shea, Jaks, STATs, cytokine signal transduction, and immunoregulation: are we there yet? *Immunity* **7** (1997) 1-11.
4. J. E. Darnell Jr. STATs and gene regulation. *Science* **277** (1997) 1630-1635.
5. T. Bowman, R. Garcia, J. Turkson and R. Jove, STATs in oncogenesis. *Oncogene* **19** (2000) 2474-2488.
6. D. E. Levy and C. K. Lee, What does Stat3 do? *J. Clin. Invest.* **109** (2002) 1143-1148
7. J. Bromberg and J. E. Darnell Jr. The role of STATs in transcriptional control and their impact on cellular function. *Oncogene* **19** (2000) 2468-2473.
8. T. Hirano, K. Ishihara and M. Hibi, Roles of STAT3 in mediating the cell growth, differentiation and survival signals relayed through the IL-6 family of cytokine receptors. *Oncogene* **19** (2000) 2548-2556.
9. S. Becker, B. Groner and C. W. Muller, Three-dimensional structure of the Stat3beta homodimer bound to DNA. *Nature* **394** (1998), pp.145-151.
10. X. Chen, U. Vinkemeier, Y. Zhao, D. Jeruzalmi, J. E. Darnell Jr. and J. Kuriyan, Crystal structure of a tyrosine phosphorylated STAT-1 dimer bound to DNA. *Cell* **93** (1998) 827-839.
11. U. Vinkemeier, I. Moarefi, J. E. Darnell Jr. and J. Kuriyan, Structure of the amino-terminal

- protein interaction domain of STAT-4. *Science* **279** (1998) 1048-1052.
12. T. Meyer, A. Begitt, I. Lodige, M. van Rossum and U. Vinkemeier, Constitutive and IFN-gamma-induced nuclear import of STAT1 proceed through independent pathways. *EMBO J.* **21** (2002) 344-354.
13. K. Melen, L. Kinnunen and I. Julkunen, Arginine/lysine-rich structural element is involved in interferon-induced nuclear import of STATs. *J. Biol. Chem.* **276** (2001) 16447-16455.
14. K. M. McBride, G. Banninger, C. McDonald and N. C. Reich, Regulated nuclear import of the STAT1 transcription factor by direct binding of importin-alpha. *EMBO J.* **21** (2002) 1754-1763.
15. T. Sekimoto, N. Imamoto, K. Nakajima, T. Hirano and Y. Yoneda, Extracellular signal-dependent nuclear import of Stat1 is mediated by nuclear pore-targeting complex formation with NPI-1, but not Rch1. *EMBO J.* **16** (1997) 7067-7077.
16. R. Fagerlund, K. Melen, L. Kinnunen and I. Julkunen, Arginine/lysine-rich nuclear localization signals mediate interactions between dimeric STATs and importin alpha 5. *J. Biol. Chem.* **277** (2002) 30072-30078.
17. J. Herrington, L. Rui, G. Luo, L. Y. Yu-Lee and C. Carter-Su, A functional DNA binding domain is required for growth hormone-induced nuclear accumulation of Stat5B. *J. Biol. Chem.* **274** (1999) 5138-5145.
18. J. Ma, T. Zhang, V. Novotny-Diermayr, A. L. Tan and X. Cao, A novel sequence in the coiled-coil domain of Stat3 essential for its nuclear translocation. *J. Biol. Chem.* **278** (2003) 29252-29260.

19. K. Nishi, M. Yoshida, D. Fujiwara, M. Nishikawa, S. Horinouchi and T. Beppu, Leptomycin B targets a regulatory cascade of crm1, a fission yeast nuclear protein, involved in control of higher order chromosome structure and gene expression. *J. Biol. Chem.* **269** (1994) 6320-6324.
20. K. Nakajima, Y. Yamanaka, K. Nakae, H. Kojima, M. Ichiba, N. Kiuchi, T. Kitaoka, T. Fukada, M. Hibi and T. Hirano, 1996. A central role for Stat3 in IL-6-induced regulation of growth and differentiation in M1 leukemia cells. *EMBO J.* **15** (1996) 3651-3658.
21. S. Imoto, K. Sugiyama, R. Muromoto, N. Sato, T. Yamamoto and T. Matsuda, Regulation of transforming growth factor-beta signaling by protein inhibitor of activated STAT, PIASy through Smad3. *J. Biol. Chem.* **278** (2003) 34253-34258.
22. Y. Sekine, T. Yamamoto, T. Yumioka, K. Sugiyama, S. Tsuji, K. Oritani, K. Shimoda, M. Minoguchi, A. Yoshimura and T. Matsuda, Physical and functional interactions between STAP-2/BKS and STAT5. *J. Biol. Chem.* **280** (2005) 8188-96.
23. R. Muromoto, K. Sugiyama, A. Takachi, S. Imoto, N. Sato, T. Yamamoto, K. Oritani, K. Shimoda and T. Matsuda, Physical and functional interactions between Daxx and DNA methyltransferase 1-associated protein, DMAP1. *J. Immunol.* **172** (2004) 2985-2993.
24. T. Yamamoto, S. Sekine, K. Kashima, A. Kubota, N. Sato, N. Aoki and T. Matsuda, The nuclear isoform of protein-tyrosine phosphatase TC-PTP regulates interleukin-6-mediated signaling pathway through STAT3 dephosphorylation. *Biochem Biophys Res Commun* **297** (2002) 811-817..
25. L. I. Davis and G. Blobel, Identification and characterization of a nuclear pore complex protein.

Cell **45** (1989) 699-709.

26. S. Bhattacharya and C. Schindler, Regulation of Stat3 nuclear export. *J. Clin. Invest.* **111** (2003), pp. 553-559.

27. A. Marg, Y. Shan, T. Meyer, T. Meissner, M. Brandenburg and U. Vinkemeier, Nucleocytoplasmic shuttling by nucleoporins Nup153 and Nup214 and CRM1-dependent nuclear export control the subcellular distribution of latent Stat1. *J. Cell. Biol.* **165** (2004) pp. 823-833.

28. C. Klebe, F. R. Bischoff, H. Ponstingl and A. Wittinghofer, Interaction of the nuclear GTP-binding protein Ran with its regulatory proteins RCC1 and RanGAP1. *Biochemistry* **34** (1995), pp. 639-647.

Figure legends

Fig. 1. **Enhanced STAT3-mediated transcriptional activation by STAT3 R214/215A mutant**

(A)(B)(C) 293T cells in a 12-well plate were transfected with STAT3-LUC (0.4 μ g) and/or indicated amounts (15–150 ng) of empty vector, expression vector for STAT3 WT (A), STAT3 RA (B) or STAT3 YF (C). Thirty-six hrs after transfection, the cells were stimulated with LIF (100 ng/ml) for additional 12 hrs. The stimulated cells were harvested, and luciferase activities were measured. The results are indicated as fold induction of luciferase activity from triplicate experiments, and the error bars represent the S.D.

(D) Hep3B cells in a 12-well plate were transfected with STAT3-LUC (0.4 μ g) together with STAT3 WT or STAT3 RA (50 or 150 ng). Thirty-six hrs after transfection, the cells were stimulated with or without IL-6 (25 ng/ml) for additional 12 hrs. The stimulated cells were harvested, and luciferase activities were measured. The results are indicated as fold induction of luciferase activity from triplicate experiments, and the error bars represent the S.D.

(E) 293T cells in a 12-well plate were transfected with ISRE-LUC (0.4 μ g) and/or indicated amounts (15–150 ng) of empty vector, expression vector for STAT3 WT or STAT3 RA. Thirty-six hrs after transfection, the cells were stimulated with IFN (50 U/ml) for additional 12 hrs. The stimulated cells were harvested, and luciferase activities were measured. The results are indicated as fold induction of luciferase activity from triplicate experiments, and the error bars represent the S.D.

Fig. 2. STAT3 RA-transfection induces enhanced phosphorylation of endogenous STAT3 and ectopically expressed STAT3 RA by LIF stimulation

(A) 293T cells (1×10^7 cells) were transfected with Myc-STAT3 WT (10 μ g) or Myc-STAT3 RA mutant (10 μ g). Forty-eight hours after transfection, cells were starved for 3 hrs, followed by treatment with or without LIF (100 ng/ml) for the indicated periods. The cells were lysed, and immunoprecipitated with anti-Myc antibody, followed by immunoblotting with anti-pSTAT3 (Tyr705) or anti-Myc antibody. Total cell lysates (1%) were blotted with anti-Myc antibody to monitor the expression of STAT3 WT or STAT3 RA.

(B) 293T cells in a 6 well-plate were transfected with Myc-STAT3WT (1.5 μ g) or Myc-STAT3 RA mutant (1.5 μ g). Forty-eight hours after transfection, cells were starved for 3 hrs, followed by treatment with or without LIF (100 ng/ml) for the indicated periods. The cells were lysed, and then immunoblotted with anti-pSTAT3 (Tyr705) or anti-Myc antibody .

Fig. 3. Subcellular localization of STAT3 WT or STAT3 RA mutant in IL-6-stimulated Hep3B cells.

(A) Hep3B cells were transfected with Myc-STAT3 WT, or STAT3RA mutant. (1.5 μ g). Thirty hrs after transfection, cells were starved for 6 hrs, stimulated with IL-6 (100 ng/ml) for 30 min, and then fixed, permeabilized with 1 % TritonX-PBS and reacted with mouse anti-Myc monoclonal antibody and rabbit anti-pSTAT3 (Tyr705) antibody, and visualized with FITC-conjugated anti-rabbit antibody and rhodamine conjugated anti-mouse antibody. The same slide was also stained

with DAPI for the nuclei staining.

(B) Hep3B cells were transfected with Myc-STAT3 WT, or STAT3RA mutant (1.5 μ g). Thirty hrs after transfection, cells were starved for 6 hrs, stimulated with IL-6 (100 ng/ml) for 30 min, and then fixed, permeabilized with 1 % TritonX-PBS and reacted with mouse anti-Myc monoclonal antibody and rabbit anti-CRM1 antibody, and visualized with FITC-conjugated anti-rabbit antibody and rhodamine conjugated anti-mouse antibody. The same slide was also stained with DAPI for the nuclei staining.

Fig. 4. Nuclear retention of STAT3 RA decreases its enhanced STAT3 activation by stimuli

(A) Quantitative time-course analysis of the subcellular localization of STAT3WT or STAT3 RA. Approximately 100 cells were classified according rhodamine signals in the cytoplasm (yellow), cytoplasm and nucleus (red) and nucleus (blue). The results represent the means of three individual experiments, in which 100 cells were counted.

(B) Hep3B cells were transfected with Myc-STAT3 or Myc-STAT3 RA (1.5 μ g). Thirty hrs after transfection, cells were starved for 6 hrs, pretreated with LMB (10 ng/ml) for 30 min and stimulated with IL-6 (100 ng/ml) for 30 min. IL-6 was then removed and the cells were incubated for an additional 4 hrs in the absence or presence of LMB, and then fixed and reacted with anti-Myc monoclonal antibody, and visualized with rhodamine conjugated anti-mouse antibody. Quantitative analysis of the subcellular localization of STAT3WT or STAT3 RA. Approximately 100 cells were classified according rhodamine signals in the cytoplasm (yellow), cytoplasm and

nucleus (red) and nucleus (blue). The results represent the means of three individual experiments, in which 100 cells were counted

(C) 293T or Hep3B cells in a 12-well plate were transfected with STAT3-LUC (0.4 μ g) and/or indicated amounts (15–150 ng) of empty vector, expression vector for STAT3 WT or STAT3 RA. Thirty-six hrs after transfection, the cells were stimulated with LIF (100 ng/ml) or IL-6 (25 ng/ml) in the absence or presence of LMB (3 ng/ml) for additional 12 hrs. The stimulated cells were harvested, and luciferase activities were measured. The results are indicated as fold induction of luciferase activity from triplicate experiments, and the error bars represent the S.D.

(D) 293T cells (1×10^7 cells) were transfected with Myc-STAT3 WT (10 μ g) or Myc-STAT3 RA mutant (10 μ g). Forty-eight hours after transfection, cells were starved for 3 hrs, followed by treatment with or without LIF (100 ng/ml) for the indicated periods. The cells were lysed, and immunoprecipitated with anti-Myc antibody, followed by immunoblotting with anti-CRM1 or anti-Myc antibody. Total cell lysates (1%) were blotted with anti-CRM1 or anti-Myc antibody to monitor the expression of CRM, STAT3 WT or STAT3 RA.

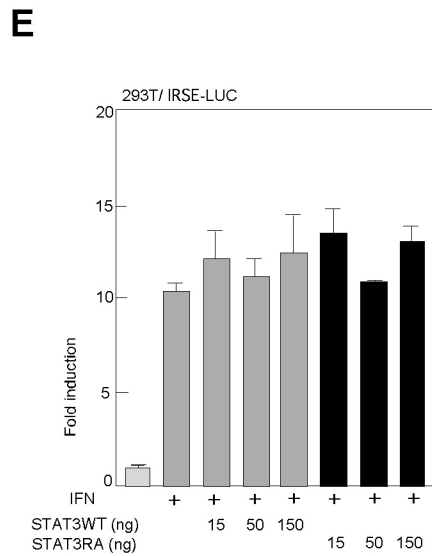
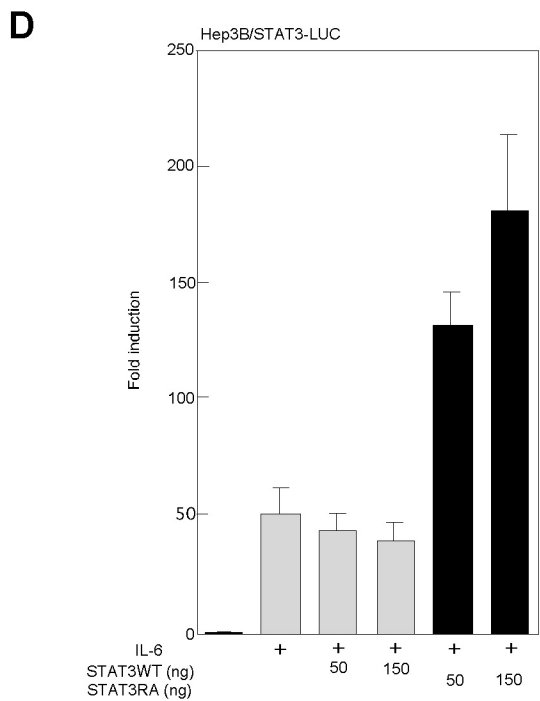
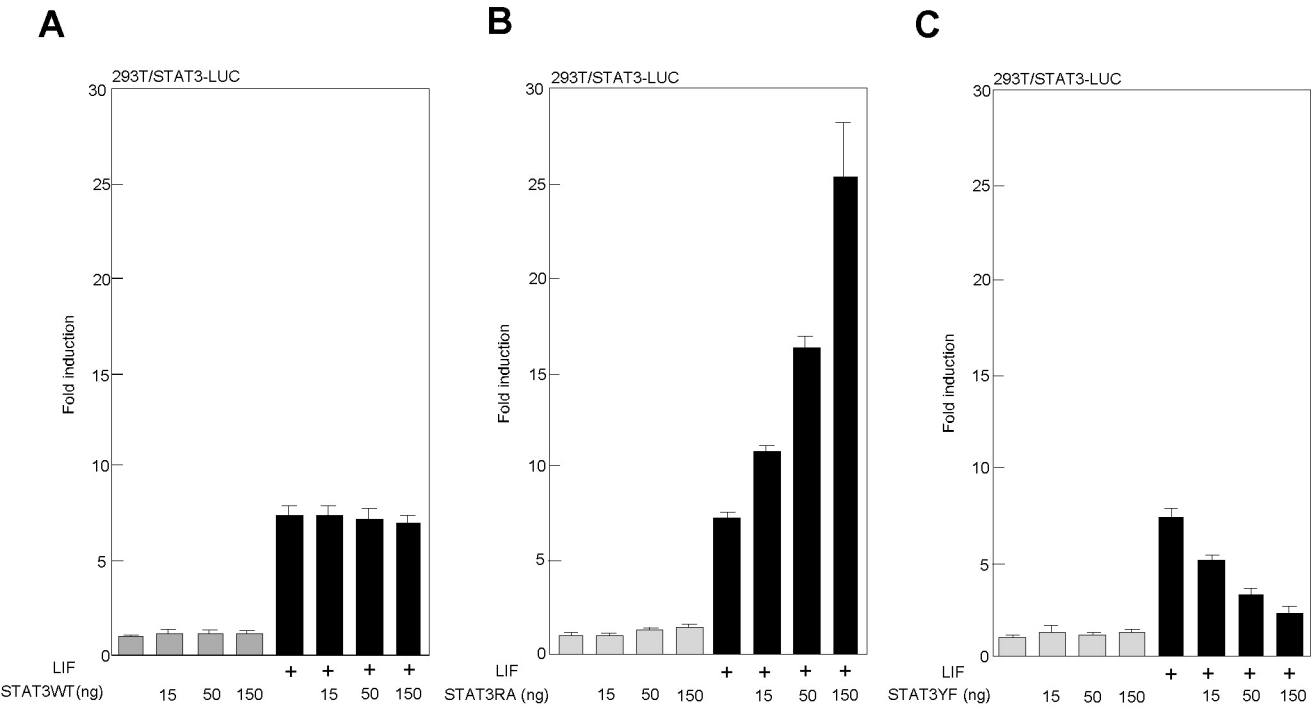
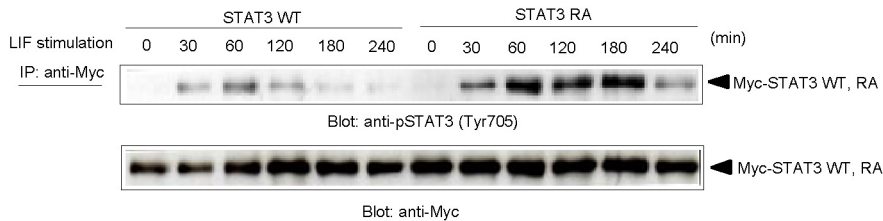
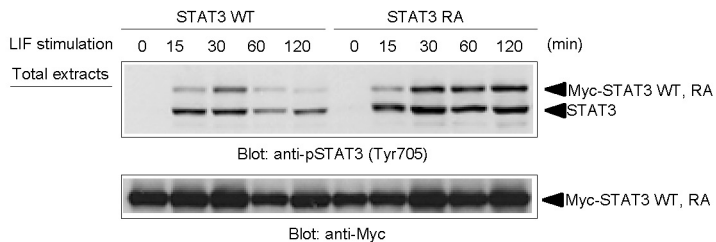


Fig. 1

A**B****Fig. 2**

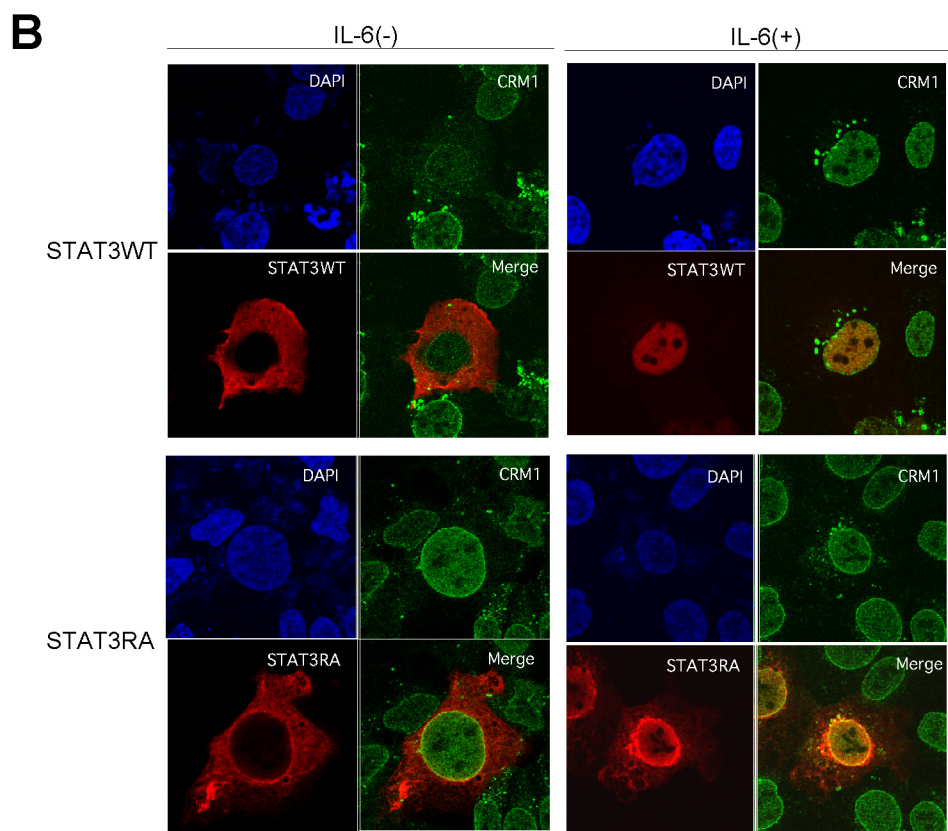
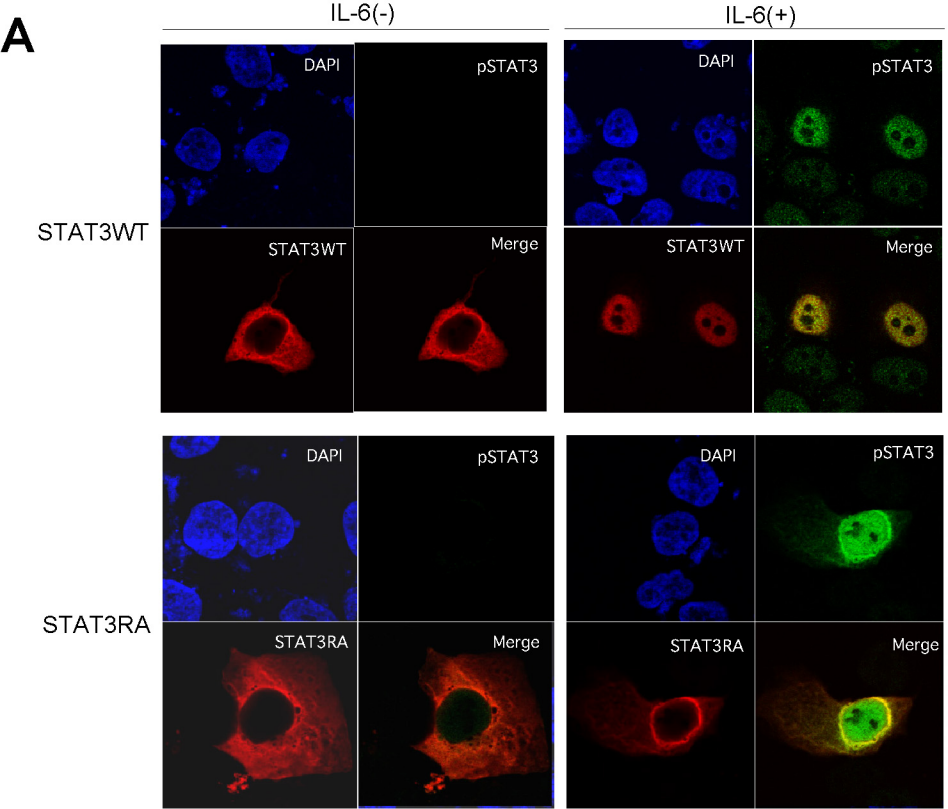
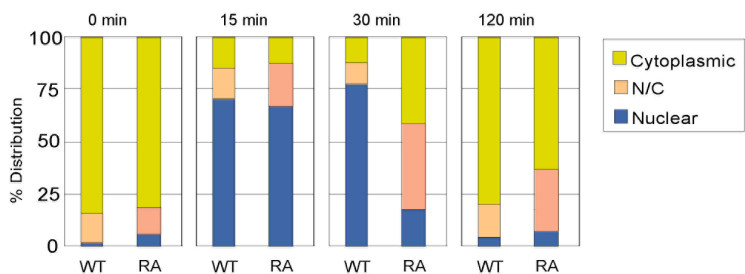
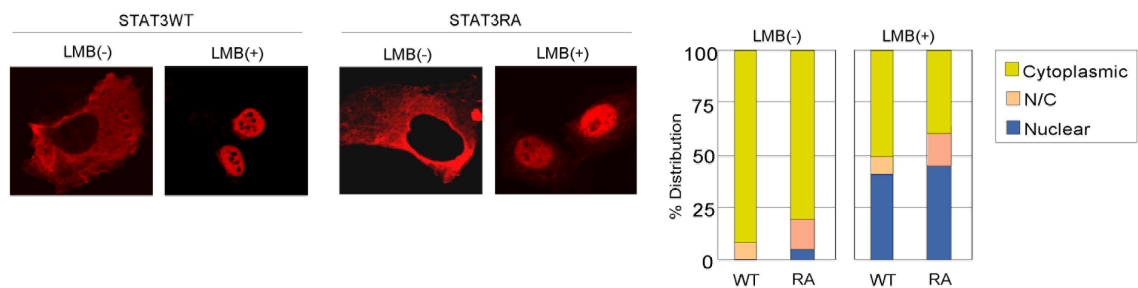
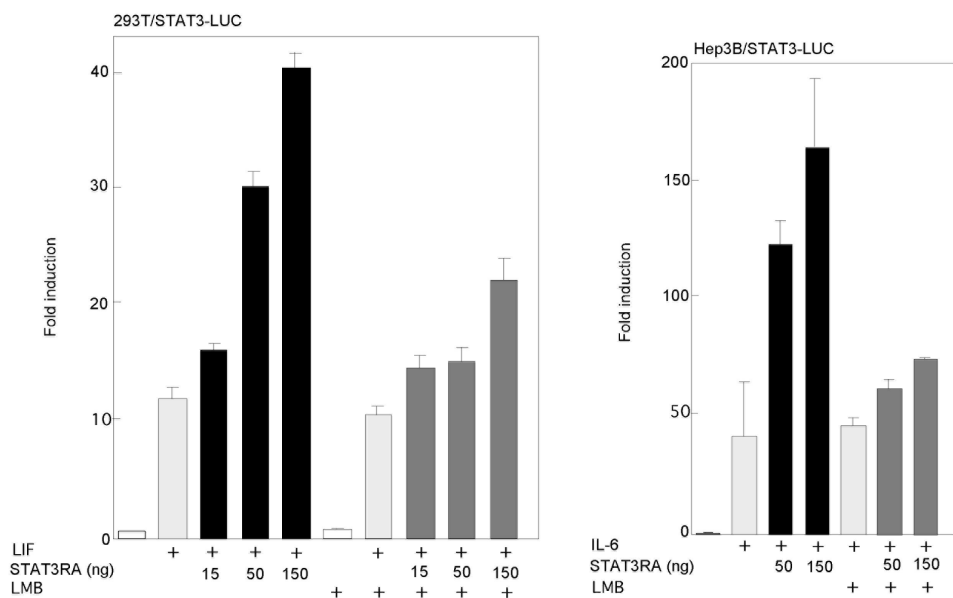
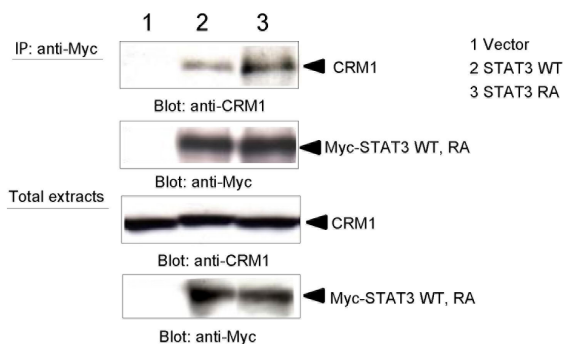


Fig. 3

A**B****C****D****Fig. 4**